

## Numerical Analysis of Swirling Jet Impingements for Thermal Management of HCPV using Nanofluids

Sajih Bin Suja\*, Md Rhyhanul Islam Pranto, Zahir U. Ahmed

Department of Mechanical Engineering, Khulna University of Engineering & Technology, Khulna-9203, BANGLADESH

### ABSTRACT

Multijunction solar cells embedded with optical elements, together known as High Concentrator Photovoltaic Module can be a solution to growing demand for renewable energy in both industrial and domestic usages. However, concentration of solar irradiance leads to high temperature leading to performance degradation of the module. For optimum performance, high concentrator photovoltaic modules need to operate within a temperature range of 110°C. Such photovoltaic modules in uncooled state may reach 1400°C under the concentration of 1000 suns. In order to overcome such challenge, an efficient cooling method is required. Thus, main objective of this study is to provide an efficient solution to this problem. In this numerical analysis, RANS based solver using SST k- $\omega$  turbulence model was adopted to analyze conjugate heat transfer problem where a moderately swirling jet impingements with flow ratio of 0.55 was implemented where two different nanofluids Al<sub>2</sub>O<sub>3</sub>-Water nanofluid and CuO-Water nanofluid was used as coolants. This proposed heat sink and flow condition lead to a reduction of cell temperature as low as 72°C for a coolant flow rate of 50 gm/min. This reduction in cell temperature further improved the electrical efficiency of the solar module under investigation.

Keywords: Photovoltaics, Jet impingements, Swirl, Nanofluids, Flow ratio

### 1. Introduction

Population growth and industrialization are forcing greater global energy demand. Fossil fuel prices are rising, but supplies are falling resulting in a growing demand for renewable energy sources. Photovoltaic (PV) solar cells are the most efficient solar technology. But of all these Photovoltaics available not all of them are efficient enough. Among them, multi-junction solar cells embedded with optical concentrators such as Fresnel lens, together known as High Concentrator Photovoltaic (HCPV) cells have been able to achieve higher efficiency compared to regular cells. However, using concentrators may be beneficial by amplifying the irradiance but such high concentration also leads to high heat zones in the solar cells that engender the issue of degrading the efficiency and structural integrity of the multi-junction solar cell [1,2]. Without a proper cooling system, such photovoltaic modules can reach up to 1200°C under a concentration of 400 suns [3]. According to Nishioka et al. [4], the efficiency of the cell decreases by 0.248% for a rise in T<sub>cell</sub> of 1°C at CR=1 and by 0.098%/°C at CR=200 with an ambient temperature of 25°C. Further, Helmers et al. [5] studied the influence of irradiance on efficiency throughout a temperature range of 5°C to 170°C and observed that efficiency decreases as temperature rises. According to Royne et al. [6], uneven cell temperature distribution leads to hot patches that shorten life spans and endanger the systems' security. Thus, thermal management is crucial for improving multi-junction solar cells' efficiency and cell quality.

For a consistent temperature distribution, passive and active cooling methods such as jet impingements, micro-channel flow, single-phase, two-phase, and phase change materials are most frequently implemented. Due to its

improved capability to enhance heat transfer inside a system, jet impingement has been one of the most widely employed techniques for cooling applications [7,8]. The jets typically impact normally on the target surface after being discharged from a circular nozzle or rectangular slots.

S. Bahaidarah et al. [9] carried out numerical and experimental methods to determine the impact of jet cooling on the photovoltaic system and reported a temperature non-uniformity of 1°C for a single solar cell. E.M Abo Zahhad et al. [2] conducted a numerical study and have also reported an acceptable reduction in cell temperature using jet impingement cooling for a coolant flow rate of 25 g/min to a maximum flow rate of 50 g/min. Jet to impingement surface is an important parameter while setting up the jet impingement system. Ansu et al. [10] from their experimental concluded that L/D=4 is an optimum range for maximizing heat transfer from jet impingement systems. Heat transfer can also be improved by increasing the nozzle diameter as reported by K. Zhu et al. [11]. However, Ikhlaq et al. [12] reported the effect of swirl and non-swirling jets for heat transfer applications. A high heat transfer area was reported and Ianiro and Cordone [13] also corroborated that with increasing swirl number, the heat transfer area increases.

Many researchers implemented nanofluids to achieve better heat transfer compared to conventional fluids. Said et al. [14] found improvement in heat transfer characteristics when nanofluids were used. Kim et al. [15] reported a 15-22% increase in convective heat transfer characteristics using alumina nanofluids for a volume fraction of 3%.

Multiple swirling jets and nanofluids can have significant effect on the thermal management of High Concentration Photovoltaic Cells, according to the literature review

\*Corresponding author. Tel.: +8801829464338

E-mail addresses: binlabib538@gmail.com

presented above. This combination has the potential to improve heat transfer and temperature distribution in HCPV. This study will compare the performance of CuO-Water and Al<sub>2</sub>O<sub>3</sub>-Water nanofluids under conditions of swirling flow.

## 2. Methodology

Ansys Workbench 2020R1 was used for analysis. The problem is a convective heat transfer problem in a thermal system embedded with a high-efficiency triple-junction solar cell, AZURSPACE 3C44 [16], with a concentration ratio of 1000 suns and swirling jet impingements, to numerically figure out how swirling jet affects the temperature of the solar cell. Commercial CFD package Ansys FLUENT 2020R1 was employed to numerically solve the problem.

### 2.1 Physical Model

In this work, a GaInP/GaInAs/Ge multijunction solar cell with an active area of 10mm10mm is subjected to a concentration ratio of 1000 suns, where each sun is 1000 W/m<sup>2</sup>. GaInP and GaInAs are utilized to produce power [8]. The board structure of this MJ solar cell is composed of two copper layers and a ceramic layer as shown in Fig. 1.

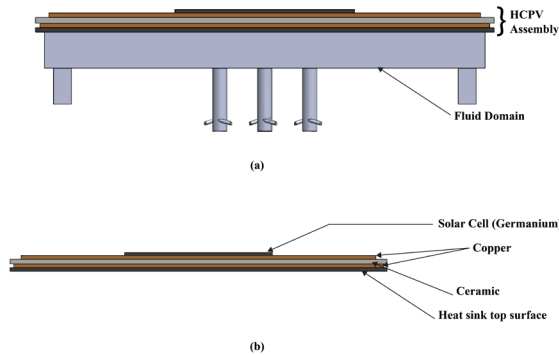


Fig. 1 (a) Computational domain for the analysis (b) Layers of the HCPV/T system.

Conventionally, such systems convert collected solar radiations to electrical power due to the photovoltaic effect, where the rest is converted to heat. To scale down the impact of the by-product of the irradiation that converted to heat a heat sink arrangement is embedded with aerodynamic swirling nozzles capable of producing swirl through the tangential ports [17] as shown in Fig. 2. Fig. 2 also depicts the other aspects of the nozzle which is modeled with three tangential ports. Coolants enter through tangential ports and axial inlets in a certain flow ratio so swirling jets can be attained. Nozzle placement in the heat sink is further provided in Fig. 3. Five nozzles were considered for the coolant flow rate. Table 1 provides assembly dimensions and other parameters involving nozzles.

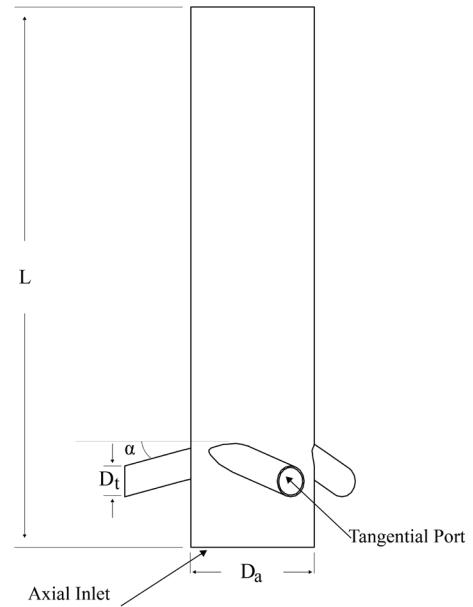


Fig. 2 Front view of the aerodynamic nozzle.

Table 1 Heat sink dimensions

Parameter	Dimensions	Parameter	Dimensions
L <sub>HS</sub>	25.5 mm	W <sub>o</sub>	1 mm
W <sub>HS</sub>	21 mm	H <sub>HS</sub>	2 mm
L <sub>o</sub>	1 mm	I	2.5 mm
L	2.816 mm	D <sub>a</sub>	0.8 mm
D <sub>t</sub>	0.2 mm	α	20°
β	15°		

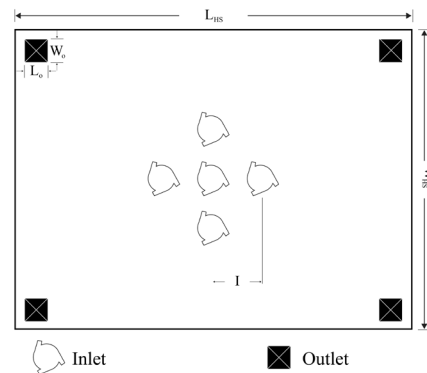
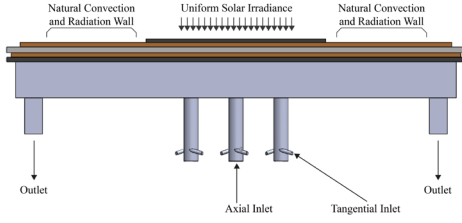


Fig. 3 Heat Sink configuration for numerical analysis.

### 2.2 Theoretical Analysis & Boundary Conditions

- The top layer of the solar cell was subjected to uniform solar irradiance.
- A mixed boundary condition (Heat loss due to convection and radiation) was applied to the free surfaces of the HCPV assembly.
- Steady-state, incompressible, and turbulent flow were adopted.

- Thermo-physical properties for the cell layers are temperature-independent.



**Fig. 4** Boundary conditions.

Inlets are considered to be mass flow inlet boundary conditions, where the mass flow rate in the axial inlet and tangential inlet are calculated from dimensionless parameter flow ratio as defined in [17]

$$Q_r = \frac{Q_t}{Q_{tot}} \quad (1)$$

Here,  $Q_{tot}$  is the total mass flow rate, which is considered to be 25 g/min to 50 g/min for the analysis.  $Q_t$  is the mass flow rate through tangential ports. Outlets condition was set to pressure outlet boundary.

### 2.3 Governing Equations

Multijunction solar cell assembly here contains several layers where heat conduction takes place and is defined according to [18]

$$\nabla \cdot (k_i \nabla T_i) + q_i = 0 \quad (2)$$

The amount of heat generated in the multijunction solar cell is calculated from [2]

$$q_{Ge} = \frac{(1 - \eta_{cell}) G \alpha_{Ge} A_{cell}}{V_{cell}} \quad (3)$$

Where  $G$  denotes net concentrated solar irradiance.

The electrical efficiency of the multi-junction photovoltaic module here is calculated according to [19]

$$\eta_{cell} = \eta_{ref} [1 - \beta_{thermal} (T_{cell} - T_{ref})] \quad (4)$$

Governing equations describing the mass conservation fluid domain are also obtained from [18]

$$\nabla(\rho_f \vec{V}) = 0 \quad (5)$$

$$\vec{V} \cdot \nabla(\rho_f \vec{V}) = -\nabla P + \nabla(\mu_f \nabla \vec{V}) \quad (6)$$

$$\vec{V} \cdot \nabla(\rho_f C_f T) = \nabla(k_f \nabla T) \quad (7)$$

Turbulence kinetic energy and dissipation of eddy viscosity in the fluid domain are described according to [20]

$$\frac{\partial}{\partial x_i} (\rho k u_i) = \frac{\partial}{\partial x_j} [(\mu + \sigma_k \mu_i) \frac{\partial k}{\partial x_j}] + G_k - Y_k + S_k \quad (8)$$

$$\frac{\partial}{\partial x_i} (\rho \omega u_i) = \frac{\partial}{\partial x_j} [(\mu + \frac{\mu_i}{\sigma_\omega}) \frac{\partial \omega}{\partial x_j}] + G_\omega - Y_\omega + S_\omega \quad (9)$$

Empirical relations specified in [21–23] were used to obtain thermo-physical properties of nanofluids. Thermal power developed was calculated and overall thermal efficiency was calculated from the equations [8]

$$\eta_{th} = \frac{Q_{th}}{DNI \cdot CR \cdot A} \quad (10)$$

### 2.4 Meshing and Numerical Setup

Meshing was done using commercial software ANSYS Mesh 2020R1 where solver preference was set to CFD and cutcell assembly meshing was employed. Proximity and Curvature were turned on.

As for solver settings, a pressure-based steady-state solver was used. SIMPLEC method was used as the pressure-velocity coupling model.

### 2.5 Grid Independency and Model Validation

For this particular analysis, grid sensitivity was carried out for  $Q_r=0$  and CuO-Water nanofluid ( $\phi=2\%$ ).

**Table 2** Grid independence test

No	No of Elements	Avg. Cell Temperature (°C)
01	387915	75.16
02	409252	73.09
03	438590	72.867
04	1487511	72.821
05	1573161	72.82

The thermal model for the analysis was validated against the numerical analysis of Cui Min et al. [3] for an uncooled multi-junction solar cell of  $3 \times 3 \text{ mm}^2$  area given in Fig. 5.

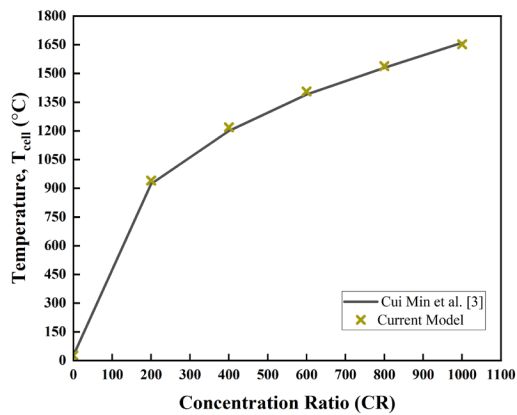


**Fig. 5** Comparison of cell temperature variation in the uncooled state for varying concentrations with numerical results of literature [3].

### 3. Results and Discussion

A graphical representation of the average cell temperature over the top layer of the solar cell is presented in **Fig. 6**. This representation is based on the mass flow rates of the coolants that were taken into consideration.

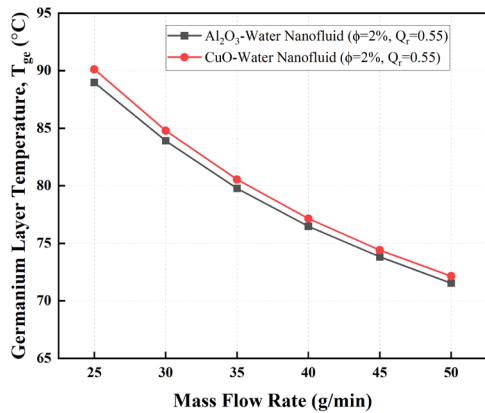


**Fig. 6** Variation of cell temperature with mass flow rates.

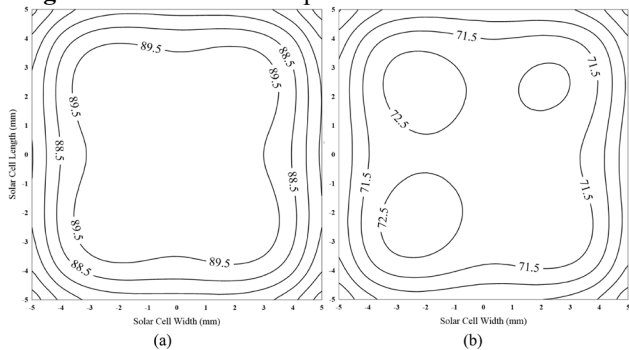


**Fig. 7** Temperature distribution on the top layer of germanium cell for  $\text{Al}_2\text{O}_3$ -Water nanofluid ( $\phi=2\%$ ) and mass flow rate of (a) 25 g/min (b) 50 g/min

In addition, **Fig. 7** and **Fig. 8** depict the local temperature contours for the maximum and lowest mass flow rates, as well as for the two alternative coolants that were utilized for the analysis of the problem. It was observed that the  $\text{Al}_2\text{O}_3$ -water nanofluid obtained the lowest temperature of  $71.538^\circ\text{C}$  at a maximum flow rate of 50 grams per minute (g/min).

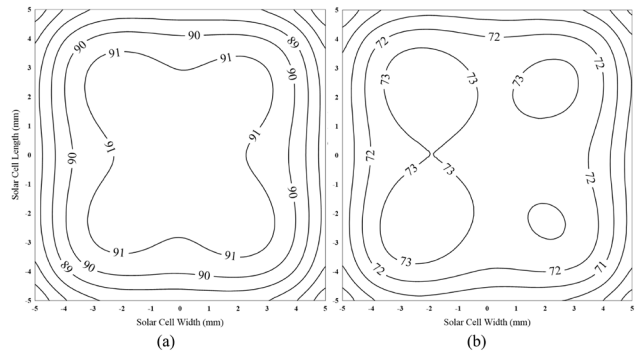


**Fig. 8** Temperature distribution on the top layer of germanium cell for  $\text{CuO}$ -Water nanofluid ( $\phi=2\%$ ) and mass flow rate of (a) 25 g/min (b) 50 g/min.

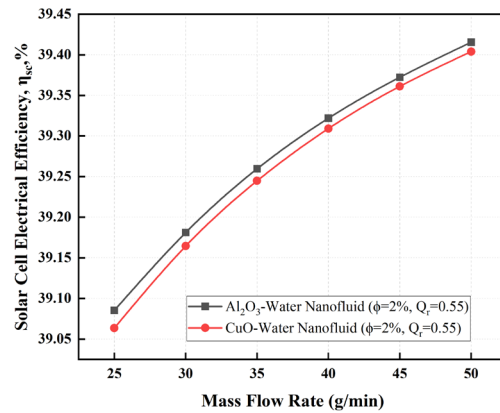


**Fig. 9** Variation of cell electrical efficiency.

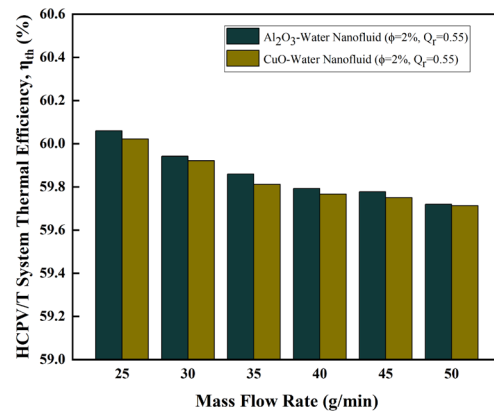


**Fig. 10** Variation of cell thermal efficiency.

The electrical efficiency of a multi-junction solar cell is represented graphically in **Fig. 8**, and the thermal efficiency of the HCPV/T system is represented graphically in **Fig. 9**, respectively. According to what was seen, increasing the mass flow rate of the coolant led to a drop in thermal efficiency, which is consistent with [2]. Even though the  $\text{Al}_2\text{O}_3$ -Water nanofluid with a mass flow rate of 50 g/min had the lowest thermal efficiency observed, it had the highest electrical efficiency. This is since when less of the solar energy is converted into heat energy, a greater amount of electrical energy is produced, which results in higher electrical efficiency.

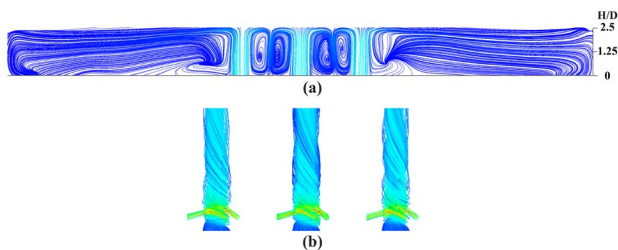


**Fig. 11** (a) Surface streamlines at  $r/D=0$  and (b) 3D streamlines at the nozzle for  $\text{Al}_2\text{O}_3$ -Water nanofluid.

**Fig. 11** (a) shows the streamline of the surface at the coordinate  $r/D=0$ . Moreover, **Fig. 11** (b) illustrates the 3D streamline of the  $\text{Al}_2\text{O}_3$ -Water nanofluid as it passes through the nozzle. A pattern that was similar to this was also seen for the  $\text{CuO}$ -Water Nanofluids. It was observed that recirculation regions emerge between adjoining nozzles when swirling flows are present for both of the coolants being used. When swirl flows are present, the streamlines can be seen to be bending and moving in an erratic pattern.

#### 4. Conclusion

In this study, the effect of swirling jet impingements on thermal management for a single high-concentrator solar cell was explored utilizing two nanofluids based on water ( $\text{Al}_2\text{O}_3$ -Water nanofluid and  $\text{CuO}$ -Water nanofluid). This study's primary purpose was to develop a solution that would provide improved temperature uniformity, improve the electrical efficiency of the photovoltaic system, and achieve a temperature that was within the manufacturer's suggested range. An acceptable temperature reduction in solar cells was seen, in comparison to the data from the uncooled state that was presented in the literature and was discussed earlier. The following is a conclusion that can be drawn from the discussions:

- Despite increases in mass flow rates, the performance of the  $\text{Al}_2\text{O}_3$ -Water nanofluid was superior to that of  $\text{CuO}$ -Water nanofluid in terms of lowering the average temperature of the cell.
- Additionally,  $\text{Al}_2\text{O}_3$ -Water exhibited superior performance in terms of achieving a higher electrical efficiency for the cell.  $\text{CuO}$ -Water

nanofluids, on the other hand, have a better thermal efficiency of the heat sink than its counterpart.

#### 5. References

- [1] M. Theristis, T.S. O'Donovan, Electrical-thermal analysis of III-V triple-junction solar cells under variable spectra and ambient temperatures, *Sol. Energy*. 118 (2015) 533–546.
- [2] E.M. Abo-Zahhad, S. Ookawara, A. Radwan, A.H. El-Shazly, M.F. El-Kady, Numerical Analyses of High Concentrator Triple-Junction Solar Cell under Jet Impingement Cooling, *Energy Procedia*. 152 (2018) 1051–1056.
- [3] C. Min, C. Nuofu, Y. Xiaoli, W. Yu, B. Yiming, Z. Xingwang, Thermal analysis and test for single concentrator solar cells, *J. Semicond.* 30 (2009) 44011.
- [4] K. Nishioka, T. Takamoto, T. Agui, M. Kaneiwa, Y. Uraoka, T. Fuyuki, Annual output estimation of concentrator photovoltaic systems using high-efficiency InGaP/InGaAs/Ge triple-junction solar cells based on experimental solar cell's characteristics and field-test meteorological data, *Sol. Energy Mater. Sol. Cells*. 90 (2006) 57–67.
- [5] H. Helmers, M. Schachtner, A.W. Bett, Influence of temperature and irradiance on triple-junction solar subcells, *Sol. Energy Mater. Sol. Cells*. 116 (2013) 144–152.
- [6] A. Royne, C.J. Dey, D.R. Mills, Cooling of photovoltaic cells under concentrated illumination: a critical review, *Sol. Energy Mater. Sol. Cells*. 86 (2005) 451–483.
- [7] M. Gharzi, A. Arabhosseini, Z. Gholami, M.H. Rahmati, Progressive cooling technologies of photovoltaic and concentrated photovoltaic modules: A review of fundamentals, thermal aspects, nanotechnology utilization and enhancing performance, *Sol. Energy*. 211 (2020) 117–146.
- [8] E.M. Abo-Zahhad, S. Ookawara, A. Radwan, A.H. El-Shazly, M.F. ElKady, Thermal and structure analyses of high concentrator solar cell under confined jet impingement cooling, *Energy Convers. Manag.* 176 (2018) 39–54.
- [9] H.M.S. Bahaidarah, A.A.B. Baloch, P. Gandhidasan, Uniform cooling of photovoltaic panels: A review, *Renew. Sustain. Energy Rev.* 57 (2016) 1520–1544.
- [10] U. Ansu, S.C. Godi, A. Pattamatta, C. Balaji, Experimental investigation of the inlet condition on jet impingement heat transfer using liquid crystal thermography, *Exp. Therm. Fluid Sci.* 80 (2017) 363–375.
- [11] K. Zhu, P. Yu, N. Yuan, J. Ding, Transient heat transfer characteristics of array-jet impingement on high-temperature flat plate at low jet-to-plate

- distances, *Int. J. Heat Mass Transf.* 127 (2018) 413–425.
- [12] M. Ikhtlaq, Y.M. Al-Abdeli, M. Khiadani, Transient heat transfer characteristics of swirling and non-swirling turbulent impinging jets, *Exp. Therm. Fluid Sci.* 109 (2019) 109917.
- [13] A. Ianiro, G. Cardone, Heat transfer rate and uniformity in multichannel swirling impinging jets, *Appl. Therm. Eng.* 49 (2012) 89–98.
- [14] Z. Said, M.H. Sajid, M.A. Alim, R. Saidur, N.A. Rahim, Experimental investigation of the thermophysical properties of Al<sub>2</sub>O<sub>3</sub>-nanofluid and its effect on a flat plate solar collector, *Int. Commun. Heat Mass Transf.* 48 (2013) 99–107.
- [15] D. Kim, Y. Kwon, Y. Cho, C. Li, S. Cheong, Y. Hwang, J. Lee, D. Hong, S. Moon, Convective heat transfer characteristics of nanofluids under laminar and turbulent flow conditions, *Curr. Appl. Phys.* 9 (2009) e119–e123.
- [16] CPV Triple Junction Solar Cell - Type 3C44C (10\*10mm<sup>2</sup>), (n.d.). <http://www.azurspace.com/index.php/en/products/products-cpv/cpv-solar-cells>.
- [17] S.M. Islam, M.T. Khan, Z.U. Ahmed, Effect of design parameters on flow characteristics of an aerodynamic swirl nozzle, *Prog. Comput. Fluid Dyn. an Int. J.* 20 (2020) 249–262.
- [18] A. Fluent, Ansys fluent theory guide, ANSYS Inc., USA. 15317 (2011) 724–746.
- [19] D.L. Evans, Simplified method for predicting photovoltaic array output, *Sol. Energy.* 27 (1981) 555–560.
- [20] M.R.I. Pranto, M.I. Inam, Numerical Analysis of the Aerodynamic Characteristics of NACA4312 Airfoil, *J. Eng. Adv.* 1 (2020) 29–36.
- [21] M. Motevasel, A. Soleimanyazar, M. Jamialahmadi, Comparing mathematical models to calculate the thermal conductivity of nanofluids, *Am. J. Oil Chem. Technol.* 2 (2014).
- [22] S. Bin Suja, M.R.I. Pranto, R.N. Turna, Z.U. Ahmed, Conjugate Heat Transfer Analysis of Different CPU Cooling Processes Using Computational Fluid Dynamics, (n.d.).
- [23] C.V. Popa, C.T. Nguyen, I. Gherasim, New specific heat data for Al<sub>2</sub>O<sub>3</sub> and CuO nanoparticles in suspension in water and Ethylene Glycol, *Int. J. Therm. Sci.* 111 (2017) 108–115.

$Q$  : Thermal power, W  
 $h$  : Heat transfer coefficient, W/m<sup>2</sup>.K  
 $\Phi$  : Volume fraction, %  
 $G$  : Concentrated Solar Irradiance  
 $\beta$  : Thermal coefficient of material

### Nomenclature

$\rho$  : Density, kg/m<sup>3</sup>  
 $v$  : Velocity, m/s  
 $C_p$  : Specific heat, J/kg.k  
 $k$  : Thermal conductivity, W/m.k  
 $\mu$  : Kinematic viscosity, kg/m-s  
 $A$  : Solar Cell Area, m<sup>2</sup>  
 $\dot{m}$  : Coolant mass flow rate, kg/s